Int J Adv Manuf Technol (2009) 41:1118–1129
DOI 10.1007/s00170-008-1560-z

ORIGINAL ARTICLE

Numerical simulation of sliding wear for a polymer–polymer sliding contact in an automotive application

Muhammad Azeem Ashraf · Bijan Sobhi-Najafabadi · Özdemir Göl · D. Sugumar

Received: 20 November 2007 / Accepted: 5 May 2008 / Published online: 5 June 2008

Abstract Injection moulded polymer-based components are important for cost effective and fast production/assembly of auxiliary mechanisms in automotive industry. Wear is one of the critical factors, which influences the reliability and useful life in such mechanical components. Experimental determination of life parameters in terms of wear has both a cost and time impact. Therefore, the ability to predict wear at the development stage enables the designers to come up with a better design, longer useful life and more reliable products. This paper presents a numerical simulation of wear for a polymer–polymer sliding surface contact in dry conditions. Finite element analysis (FEA) is used as a tool to calculate nodal pressures at the contact area for small sliding steps. These pressures are then inputted to a customized wear calculating routine. The routine uses averaged wear coefficients (wear rates) obtained from custom designed experiments. The FE contact geometry is modified after each sliding step to account for the contact height decay thus determining wear volume loss over usage time and predicting the worn geometry.

M. Azeem Ashraf (✉) · B. Sobhi-Najafabadi · Ö. Göl
School of Electrical and Information Engineering,
University of South Australia,
Mawson Lakes, SA 5095, Australia
e-mail: MdAzeem.Ashraf@postgrads.unisa.edu.au

D. Sugumar
Centre for Materials and Fibre Innovation, Deakin University,
Geelong Campus,
Warurn Ponds,
3217 Victoria, Australia

Keywords FEA · Wear · Sliding contact · Nodal solution nodal pressure

1 Introduction

Sliding contacts, whether in rotary or linear manner, exist almost in any mechanical system. Over usage, as a result of friction, the mutually sliding surfaces of such contacts will experience material removal known as wear. This changes the effective geometry and the dimensions of the mating components, thus effecting useful life of the components and hence the product. Experimental determination of life parameters in terms of wear has both cost and time impact [1]. The ability to simulate wear and consequent useful life prediction can benefit product designers and manufacturers in multiple manners as, designing better products, contemplating better maintenance plans to avoid potential failures and avert financial losses. Some of the application areas where wear simulation can augment design are but not limited to: sliding or rotating components in automotives, engines and pumps, consumer products, prosthetic joints and lately MEMS-based micro machines [2, 3].

The finite element analysis-based (FEA) wear simulation and life prediction methodology presented in this research can be leveraged to any of the aforementioned areas. However due to the availability of industrial and consumer experience data, manufacturing facility and experimental setup to verify the simulations, the sliding joint of an automotive rear view mirror was selected for a pilot study. Subsequent sections narrate formulation useful life prediction problem based on the said product.

Therefore, the ability to predict wear at the development stage enables the designers to come up with a better design, longer useful life and more reliable products. Although this

situation may occur any contact mechanism this research focuses on a folding–unfolding mechanism existing in an automotive rear view side mirror assembly.

2 Background

The importance of a side rear view mirror while driving a car cannot be denied. As illustrated in Fig. 1, the actual mirror is mounted on the car body with the help of two subassemblies. Sub-assembly 1 mounts to the car body and the sub-assembly 2, which houses the mirror, has a swiveling joint with sub-assembly 1. In order to reduce hazard of protruding obstruction to pedestrians and reduce parking space, many of the modern cars have the feature of closing (manual or motorized) the mirrors upon parking. Fig. 1 indicates the two extreme positions for swiveling of sub-assembly 2 as 'opened' and 'closed'.

An exploded 3D assembly drawing of the swiveling joint correlating the sliding contacts to a picture of unworn joint is illustrated in Fig. 2, whereas the isolated geometry details of the sliding contact at the swiveling joint are depicted in Fig. 3. The 'base' is the part of sub-assembly 1 and is fixed, where as the 'slider' forms a part of sub-assembly 2 and is free to slide on the Base. The three detents loaded with a compression spring (indicated with normal forces applied) provide stability to the mirror mounting against vibratory motion resulting from engine and car movements. Due to repeated opening and closing action of sub-assembly 1, detents of the slider experience wear or material loss, this alters the dimension at the joint. Wearing of the detent heights beyond a safe performance threshold result in excessive vibrations being transmitted to the mirror and hence distorting the image viewed. Such image distortion due to vibrations is one of the failure modes for the mirror assembly. A prediction of detent wear rate and, hence, the useful life of the sliding joint can provide important design and maintenance information.

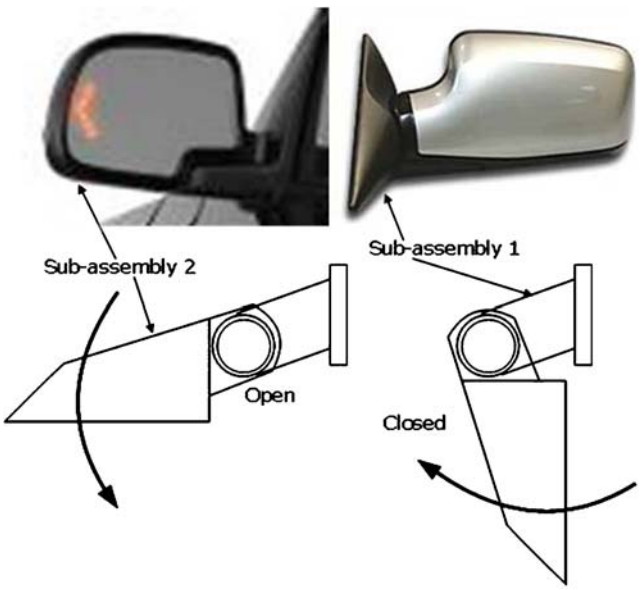

Fig. 1 Rear-view mirror with extreme positions

Subsequent sections cover an introduction to sliding wear, a systematic and comprehensive wear modeling methodology followed with a numerical simulation of sliding wear for the said joint.

3 Sliding wear

Wear in mechanical components can be attributed to a number of factors like geometry of contact surfaces, applied loads, sliding speed, material hardness, and friction characteristics. Given these varying nature of these factors, wear phenomenon can be treated as a dynamic process [4, 5] and prediction of that process can be considered as an initial value problem. The wear rate may be described by a general Eq. [6]:

$$\frac{dh}{ds} = f(load, temperature, sliding\ speed, material\ properties, surface..) \quad (1)$$

where *'h'* represented the wear depth and 's' is the sliding distance. There are over 300 wear models presented in tribology literature, with mathematical expressions varying from simple empirical relationships to complicated equations relying on physical concepts and definitions. Yet, no single predictive equation or group of limited equations could be found for general and practical use [5].

The most frequently used model in wear is the linear wear model, presented in mid-1900s and usually referred to as the Archard & Rabinowicz wear model [6, 7]. The model was based on experimental observations where volume wear rate is proportional to the nominal normal load, and assumed softer of the two contact surfaces to wear. The following section describes the said model.

3.1 Archard's wear model

Archard and Rabinowicz introduced "wear coefficient", K, as a quantity of fundamental importance in any wear calculation [7, 8]. Determination of wear coefficient is the first step in a wear analysis, defined as

$$K = \frac{3HV}{Pd} \quad (2)$$

V, P and d are wear volume, normal force and sliding distance, respectively. H is Brinell hardness of the material

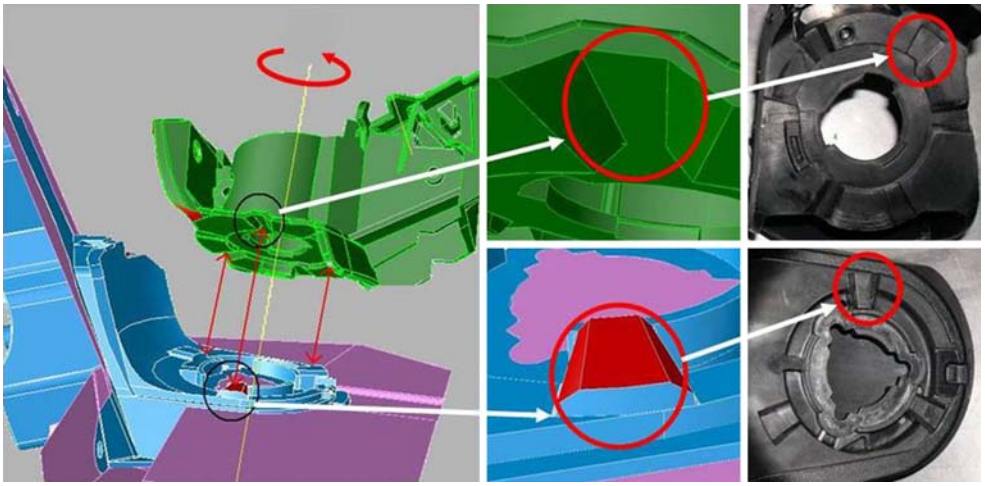

Fig. 2 Exploded assembly view of the swiveling joint

[9]. Pin-on-disc experiments are performed to obtain the wear coefficient.

Wear depth '*h*' for a dimension is a more accepted design parameter in engineering applications as compared to wear volume. An alternate form of Archard's wear equation can be used to directly calculate '*h*';

$$h = kpd \tag{3}$$

where k is the dimensional wear coefficient (Pa^{-1}), p is the normal pressure (Pa) and d denotes the sliding distance (m) [6].

4 Wear of mirror swiveling contact

Figure 4 illustrates a close up of new and worn contact surface for one of the sliding contacts depicted earlier in Figs. 2 and 3. In order to get a picture of how the contact wear is progressing with cycles of usage, periodic inspections of contact area are necessary. However, as the contacts are concealed in the mirror assembly (Fig. 1) during operation, disassembling and reassembling the unit for each observation will alter the orientation giving erroneous results and hence is not feasible.

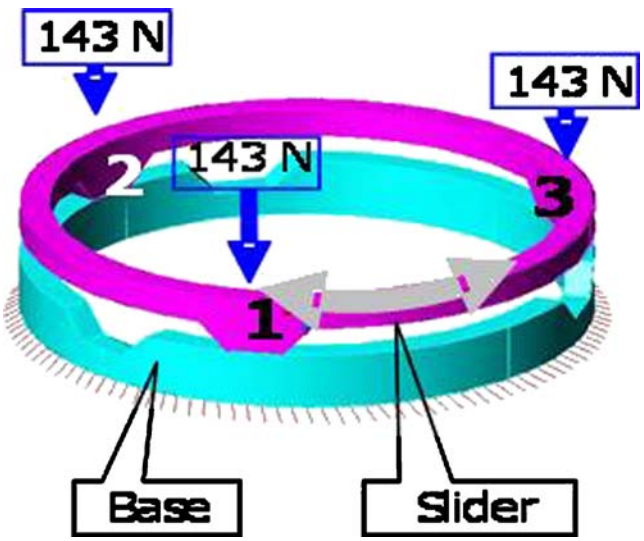

Fig. 3 Sliding contact at the swiveling joint

However an indirect measure of wear effect was devised in form of 'folding force' (FF). FF is defined as the force required to push the mirror to either open or close positions, as depicted in Fig. 1. This force will gradually diminish depending on the condition of the contact geometry. Figure 5 presents the results of monitoring FF over cycles of usage. As illustrated in Fig. 5, a new joint is firm with no wear requires a higher folding force; however, a worn joint with sliding edges beveled requires lesser folding force. Inspection of the samples at the beginning and end of the test reveals a wear situation similar to Fig. 4 and evidences the FF decay depicted in Fig. 5. Moreover, the diminishing folding force effect observed by the end user would be an unstable rear view mirror with a vibrating image, which indeed causes visual discomfort for the driver.

5 Wear simulation methodology

Although there are over 300 wear models presented in tribology literature, a general wear model applicable to all situations is still not available [10]. Thus, effective wear prediction requires a suitable analytical wear model tailored to meet the design in consideration, which can then form the basis for any numerical simulation of wear. Therefore, initial experiments are necessary to adapt the models to wear scenario under consideration [11].

In the absence of well-established wear modeling procedures a systematic wear simulation was proposed by Ashraf et al. [11], the same is used in this research to

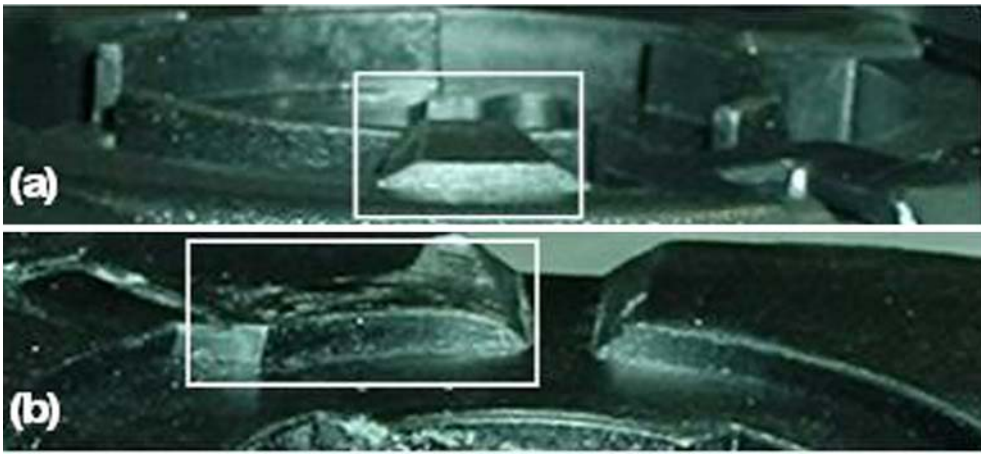

Fig. 4 (**a**) Actual contact with no wear (**b**) Actual contact with wear

develop the numerical simulation from initial experiments and analytic model. Figure 6 depicts the systematic wear simulation approach.

At macro level wear modelling can be classified into three major activity groups, with *initial experimentation* preceding *analytical* and *numerical modelling*. A detailed explanation of individual steps can be found in author's work [11]. Based on the tribo-system analysis and initial experiments [12, 13], Table 1 presents key wear parameters to be used in subsequent modelling for the two parts involved.

5.1 Experimental setup

To achieve realistic wear coefficient values and later a wear prediction model for the case detailed earlier, a customized experiment setup designed based on the pin-on-disc wear testing standards was designed [G 98 standard for wear testing]. The experimental contact geometry was designed to mimic the geometry of the real contact as it appears in the final product. Figure 7 depicts experimental setup and the actual joint geometry consisting of three sliding contact pairs.

Referring to Fig. 7 base is used as the disc and the 'slider' correspond to pin when it is compared to conventional pin-on-disc method. 'slider' is mounted on a rotary pneumatic cylinder, which can be revolved in clock and anti-clock wise directions relative to the fixed base. It consists of three contact pairs. There is a 430 N dead load applied on the slider as the normal load, which is assumed to be equally distributed across each of the three contact pairs (~143 N). The angular stroke of the slider is 32.3° as

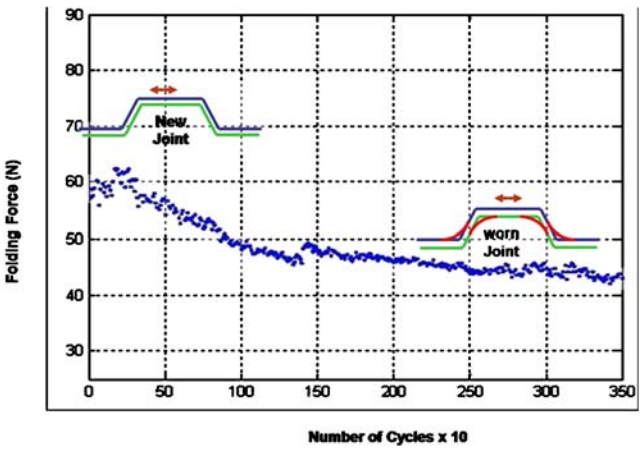

Fig. 5 Decay in folding force over usage cycles (Source: Lab tests of the joints at Schefenaker Australia (SVSA)

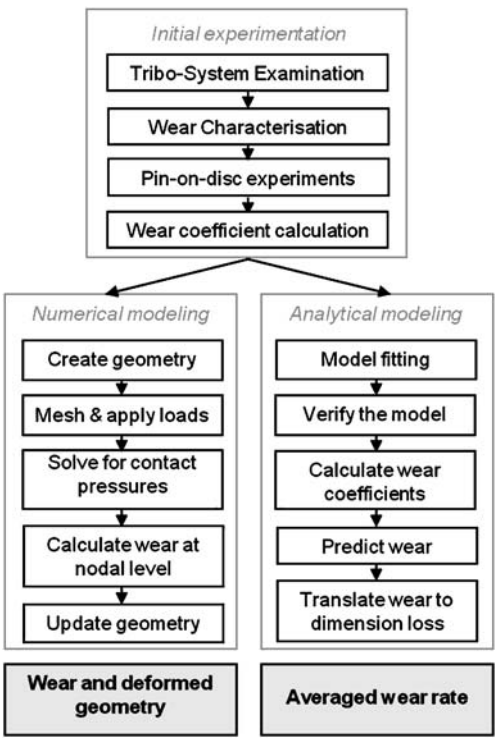

Fig. 6 Wear simulation approach

Table 1 Test setup principle data

Material properties	
Slider	Material: BK159 45% glass reinforced modified polyethylene terephthalate Density: 1700 kgm^{-3} Tensile strength: 186 MPa Commercial name: Rynite 545 NC010 by DuPont
Base	Material: 33% glass reinforced, heat stabilised black nylon copolymer resin Density: 1400 kgm^{-3} Tensile strength: 172 MPa Commercial name: Zytel 72G33HS1L by DuPont
Sliding parameters	
Coefficient of friction	0.17
Experimental coefficient of wear	0.000071329

defined by the operating range of the mechanism. Thus the linear sliding distance can be computed for wear volume loss calculations. The principle data of material and test setup are listed in Table 1 [13].

6 Finite element method-based wear simulation

So far none of the commercial FEA-based design and analysis softwares provide an integrated wear simulation tool. However, using the available contact analysis tools, indirect wear estimation approaches are proposed to estimate wear [6, 14]. Implementation of any such approach depends on the openness and the capability of FEA software to incorporate external algorithms. This section presents contact analysis in FEA and implementation of wear algorithm.

Contact analysis in finite element method (FEM) is a nonlinear problem. Contact stresses and contact pressures are the two main quantities sought in FEM-based wear simulation. The continuous and random dimensional

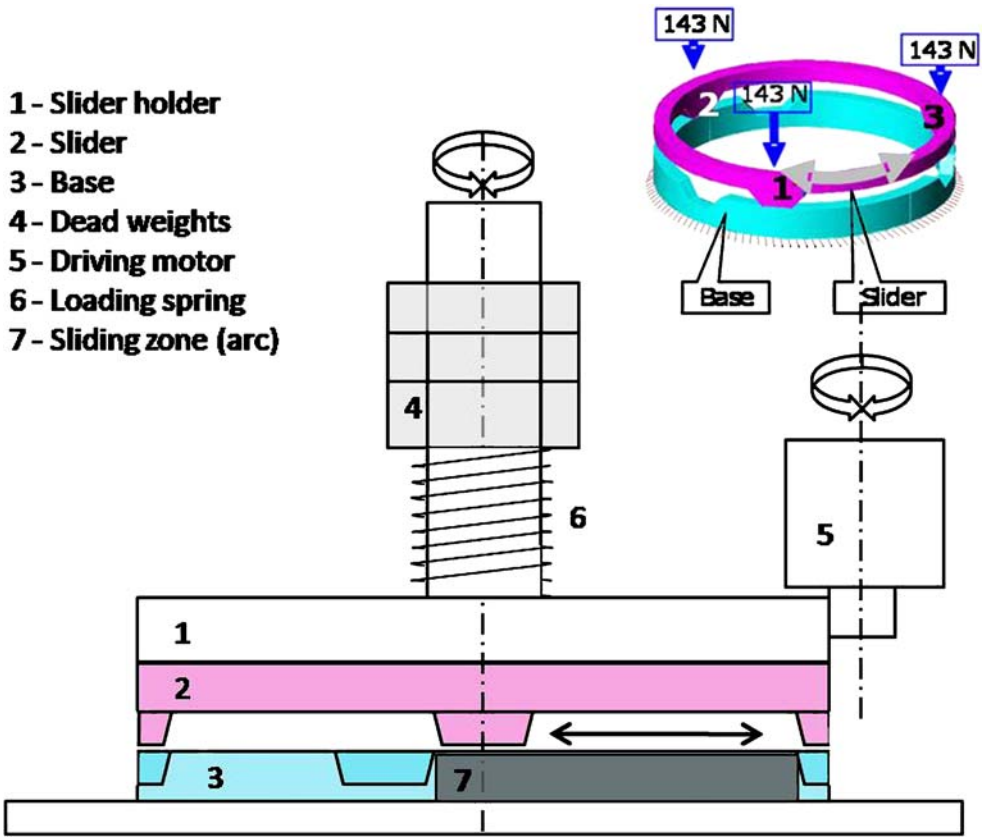

Fig. 7 Wear testing setup specific to research problem

change of wear surfaces poses a significant difficulty in sliding wear problems. Their shapes vary due to the sliding velocity, load, material parameters, and surface topographies, and will be changed as a result of the friction and wear. The important wear modeling task is the ability to obtain precise amount of worn material out of any sliding situation and for any geometry [15].

ANSYS, the commercial FEA software used for this research can handle several material and structural nonlinearities, i.e., plasticity, viscoelasticity, and friction. For contact problems, ANSYS can model contact condition with different types of contact element and present Lagrange multiplier, penalty function and direct constraint approaches. When meshing a model, the nodes on potential contacting surfaces comprise the layer of contact elements whose four Gauss integral points are used as contacting checkpoints [16].

6.1 Wear simulation algorithm

The finite element method (FEM) gives the flexibility of solving the sliding contact wear problem at element level for successive small sliding intervals. Modifying the geometry after each step to incorporate wear includes the dynamic effects of material removal in subsequent steps. Selection of an appropriate sliding step is important for the accuracy of the results, which is discussed later.

Contact analyses tools are used to solve sliding contact as a series of successive static load problems. After each sliding step nodal pressures at the contact nodes of the wearing member are extracted (recall the assumption made earlier that only softer of the two members would wear). Derivation of Archard's wear law depicted in Eq. 3 is applied to calculate nodal wear in vertical axis. The FEM-based stepwise sliding wear calculation algorithm used in this research is presented in Fig. 8. Initially each node is moved individually, thus instigating the localized material removal. The distance moved by the contact node may not be uniformly distributed along the sliding surface. This not only leads to the prediction of height decays of the contact, but also indicates the approximate worn shape [6, 14].

However, after a few iterations, when the cumulative displacement of any contact node nears the element height, further movement of nodes destabilizes the FEA model. In this case a revised geometry of the worn contact has to be defined. The element height, thus, mentioned depends on this choice of FEA software, meshing size, and element types used in the model.

6.2 Finite element model

Figure 9 illustrates the FE model for one of the three detents depicted in Fig. 3. To simplify the problem it is

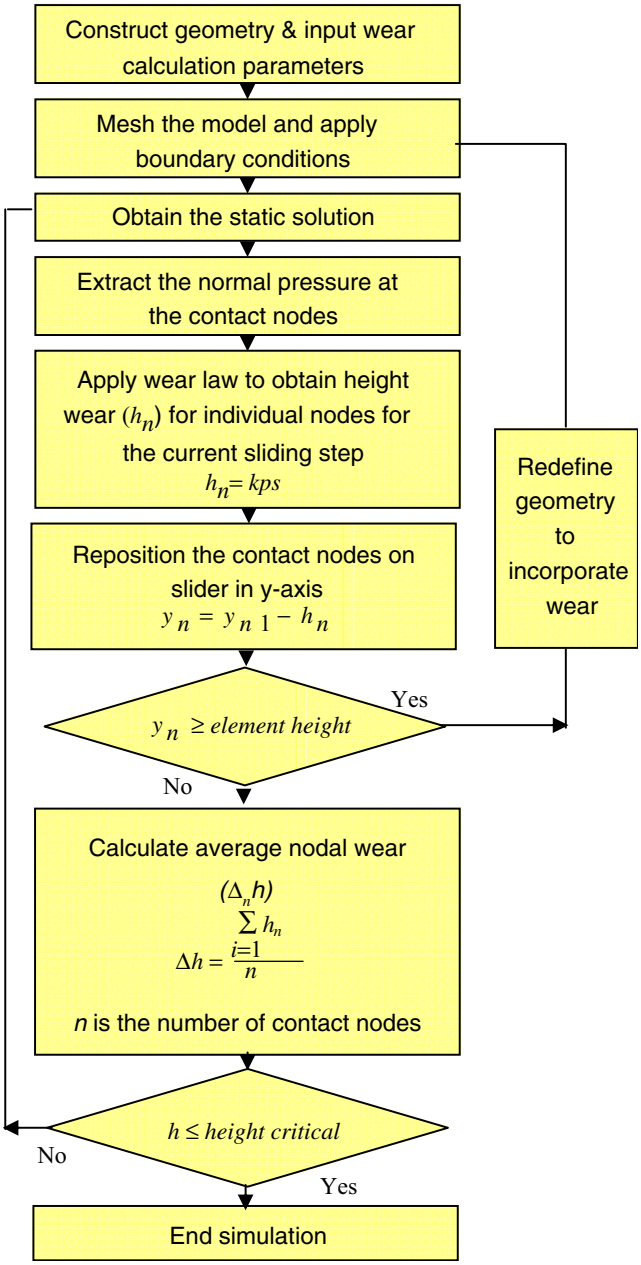

Fig. 8 Wear calculation algorithm with individual nodal displacement

assumed that all three detents experience uniform and simultaneous wear. The problem is reduced to a two-dimensional model with the assumption that wear would be uniform along the 3rd Cartesian dimension (depth). In the figure, slider and base are trapezoid and rectangle, respectively. A uniform pressure is applied on top of the slider with displacement (sliding step) in x-axis. The sides of the base are constrained in all degrees of freedom to prevent rigid body motion.

For the stability of surface-to-surface contact FEA model, it is mandatory that neither of the mating surfaces penetrate into each other. For this purpose ANSYS

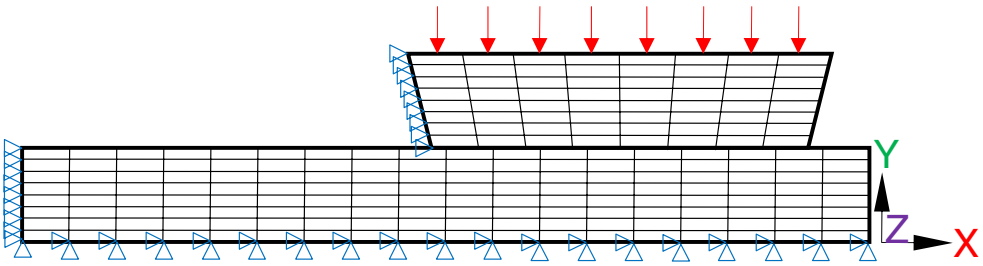

Fig. 9 Two-dimensional contact model with boundary conditions

classifies the two surfaces as contact and target with specific element types assigned to each, namely CONTA171 and TARGE169. Actual location of the contact depends on the geometry of the mating surfaces; ANSYS uses augmented Lagrangian formulation to find the contact regions. The model is limited to experience small deformations only. The structural equilibrium is found by incrementally changing the applied load. A converged solution is reached after a few Newton–Raphson iterations [16].

6.3 Sliding step size determination

The model presented above is solved for different sizes of the sliding step. Internally each sliding step is divided into a number of sub-steps. The nodal pressure distribution for the contact nodes is plotted for each sub-step in Fig. 10. It can be seen as the step size is increased the pressure distribution starts varying considerably. This behaviour of FEA model affects the overall solution. Although a model solved with a smaller sliding step gives more accurate results, it comes at the expense of computational time. Therefore, the solution step is to be selected accordingly. In this case, the solution step of 0.1 mm was used.

The model presented above is solved for different sizes of the sliding step. Internally each sliding step is divided into a number of sub-steps. The nodal pressure distribution for the contact nodes is plotted for each sub-step in Fig. 10. It can be seen as the step size is increased the pressure distribution starts varying considerably. This behaviour of FEA model affects the overall solution. Although a model solved with a smaller sliding step gives more accurate results, it comes at the expense of computational time. Therefore, the solution step is to be selected accordingly. In this case, the solution step of 0.1 mm was used.

7 Numerical results

There are two key outcomes expected from an FEA wear analysis: height decay and worn geometry. Height decay over time gives an estimation of the component life, whereas the worn geometry gives an insight to the design's weak spots susceptible to wear. Added to the above two factors, 'sliding contact wave propagation' over the sliding steps is also presented.

To simulate the actual to and fro motion of the actual product, sliding distance was translated to repeated back and forward sliding strokes. The sliding stroke is FEA model illustrated in Fig. 9 was solved for repeated sliding steps. Due to the limited computational capability and development support from the FEA software used, we were not able to run the simulation for the complete number of sliding steps summing to the overall sliding distance of 400 meters. However, a reasonable accuracy was achieved with the assumption that the wear outcome remains unchanged for 100 successive sliding steps. At each 100 sliding step the cumulative height decay was incorporate in the FEA model and solved for next 100 steps.

7.1 Contact pressure analysis

Pressure distribution and contact status for the first sliding step solution for the contact problem are illustrated in Fig. 11(a) and (b), respectively. From Fig 10(a) it can be seen the pressure is distributed evenly at the middle region of the contact whereas the edges have maximum pressure concentration. This evidences that wear would be initiating from the contact edges. Ansys classifies the contact status as 'near contact' and 'sliding', which are denoted by different color in Fig. 11(b). The figure shows that the full face of the *slider* is in sliding contact. This initial contact will be converted to unevenly distributed small contact regions after few steps of wear as illustrated in the following results.

Subsequent to the first contact solution step mentioned above, the contact is solved for the second sliding step by incorporated wear calculated from the above solution (refer to Fig. 7), which is shown in Fig. 12. Figure 12 is of marked significance in wear visualization. Referring to Fig. 12(a) & (b) there is no sliding contact at the edges and the contact is reduced to a small region for which the pressure distribution is indicated. This is indicative of wear on both edges that conform to the conclusion from the previous step, .i.e., wear would be initiated from the edges of the sliding contact.

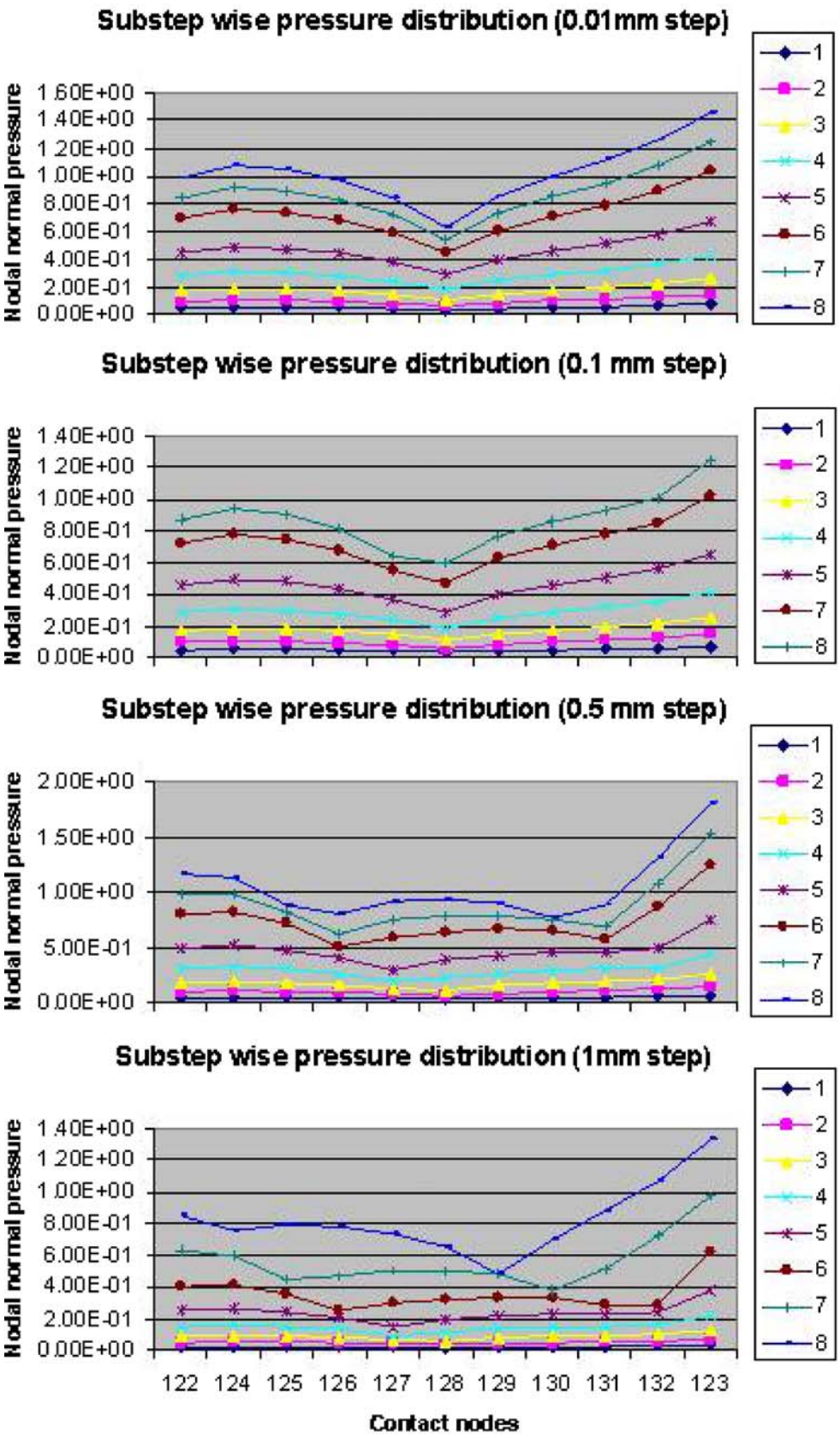

Fig. 10 Pressure variation with sliding step size

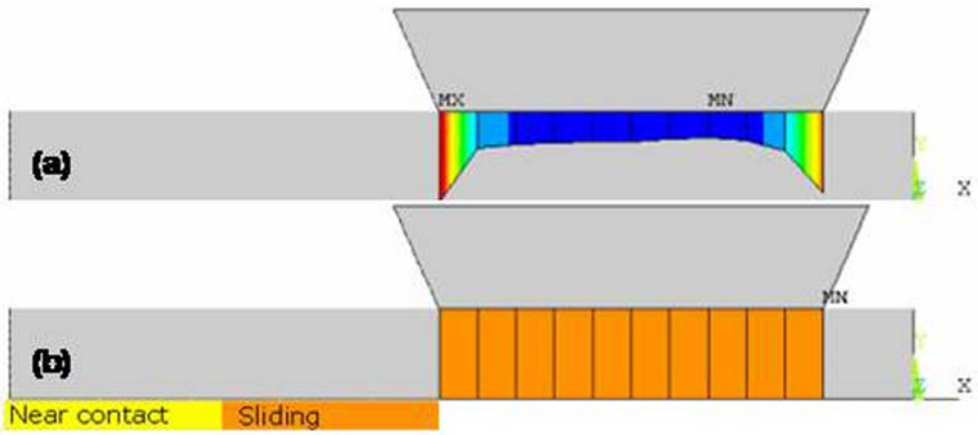

Fig. 11 (**a**) first step pressure distribution, (**b**) contact status

7.2 Contact sliding wave

Due to the elastic nature of polymers, the initially contacting surfaces do not maintain an absolute contact while sliding on top of each other The initially flat contact (as exhibited in Fig. 11(b)) becomes a series of detachment waves also known as Schallamach waves moving along the contact zone during sliding [17, 18]. This phenomenon was observed during successive contact solutions. The oscillatory motion of the contact zone is now addressed.

After incorporating first wear, the resulting contact is solved for the sliding step. Internal to the FEA software, each sliding step is divided into ten sub-steps. Analysis of the solution result at these sub-steps reveals the shifting of sliding contact zone along the face of the *slider*. This conforms to the wave phenomenon described above. Using the Ansys classification of contact status, we find that Fig. 13 indicates the traveling of the actual contact zone along the face of *the slider*.

Referring to Fig. 4, the vertical line on the right indicates the starting datum for x-axis motion of the slider. A localized pressure distribution with the shape of two conjoined triangles for each sub-step indicates a very small contact detachment not physically visible on the scale of the drawing. A contact separation travel opposite to the direction of the sliding can be seen in successive sub-steps 3, 4 and 5. Since the above data was obtained after incorporating a few iterations of wear, the wave encounters a cavity, resulting from the material removal, causing a contact gap terminating the wave in step 5. In Fig. 4, the wave can be seen to follow a cyclic pattern in sub-step groups of {3,4,5}, {6,7,8} and {9,10,11}.

7.3 Wear calculation

The accumulated wear of *slider* becomes visible after 50 iterations. Figure 14(a) and (b) illustrate a comparison of the initial (no wear) geometry and a worn geometry of the contact after 50 iterations. It is obvious that the leading and trailing edges are experiencing more wear than the remaining contact area. This result conforms to the wear pattern in actual prototype units shown in Fig. 14(c) & (d).

These result in Fig. 14(b) indicate the accumulated wear for 50 iterations. Intermittent worn geometries may differ from the one presented. However, the analysis can be

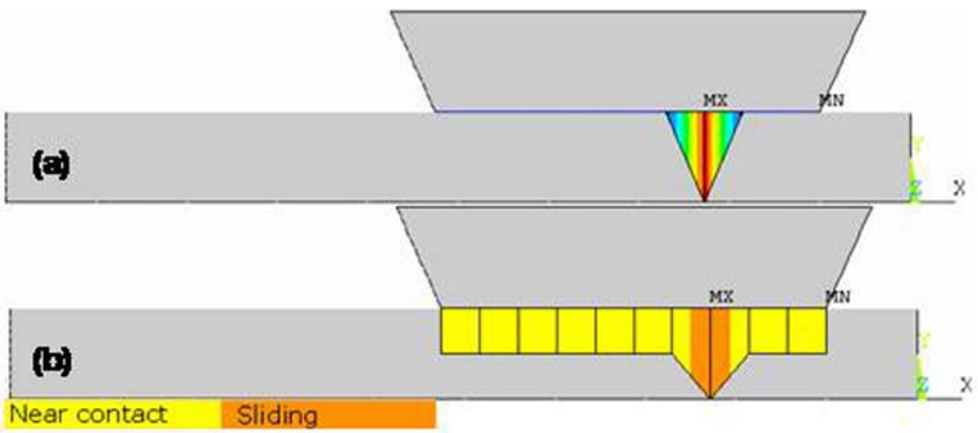

Fig. 12 (**a**) Pressure distribution after first wear step, (**b**) Sliding contact after first wear step

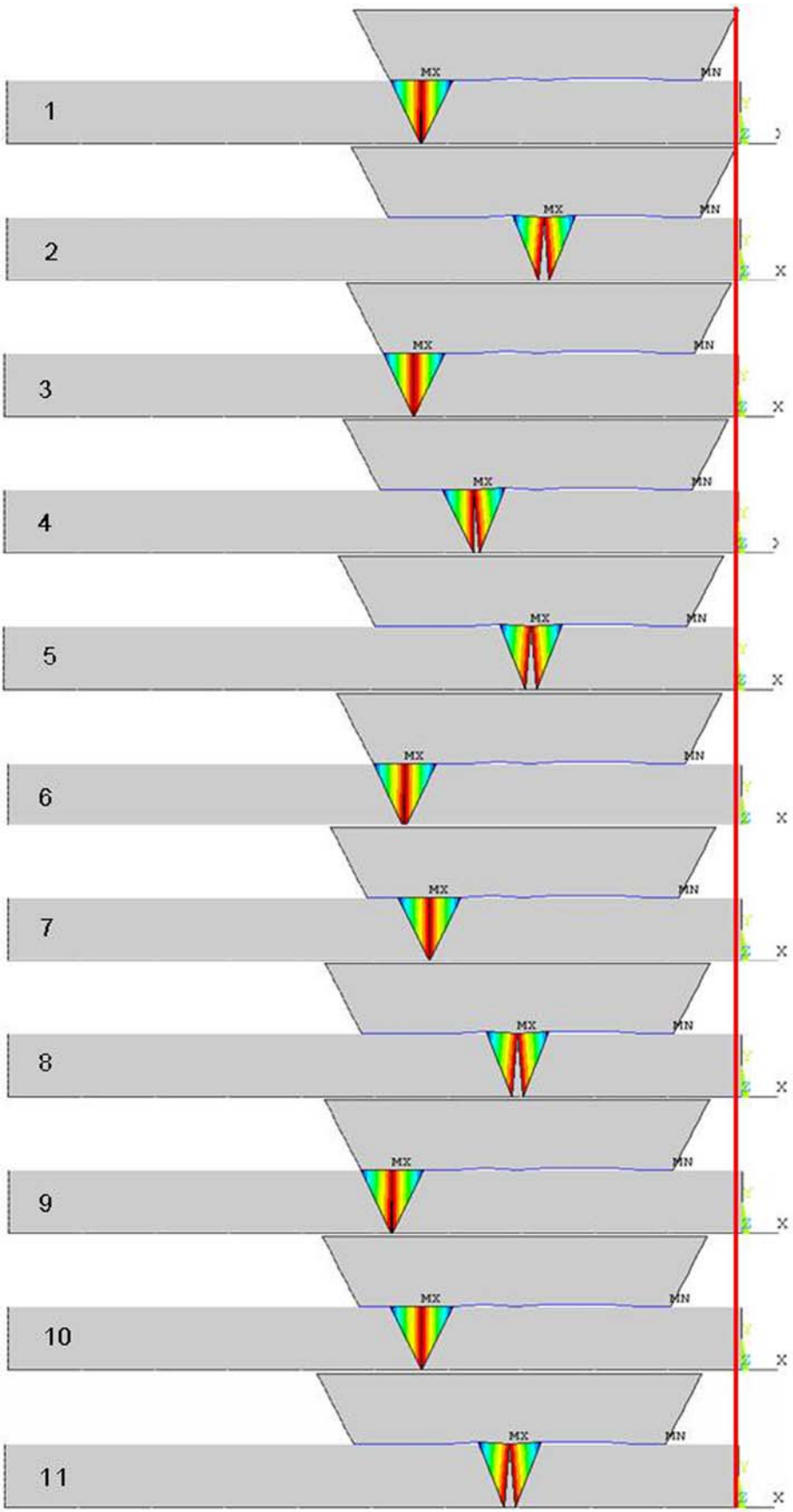

Fig. 13 Travelling of contact detachment wave

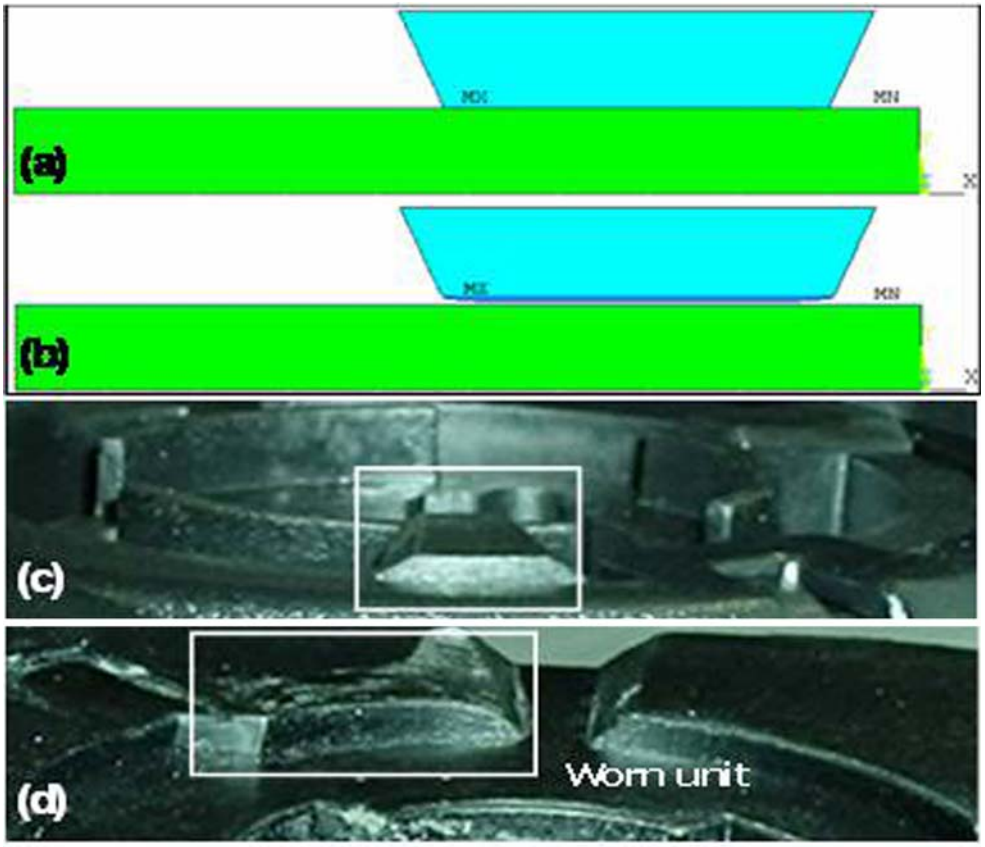

Fig. 14 (**a**) No wear geometry, (**b**) Worn geometry from FEA results, (**c**) Actual product with no wear, (**d**) Actual product with wear

stopped at any intermittent stage to observe the wear progression corresponding the accumulated sliding distance

7.4 Accumulated dimension loss

Finally, the height decay over cumulated sliding distance results for *slider* extracted from FEA solutions measured data and analytical calculations are presented in Fig. 15. It can be seen that FEA-based results are in close proximity of the experimental values. This proves the validity of algorithm and the modeling approach.

8 Discussion and conclusion

Although the problem presented operates on a plane on plane sliding problem. However, the wear-solver section of the algorithm extracts and operates on boundary layer nodes

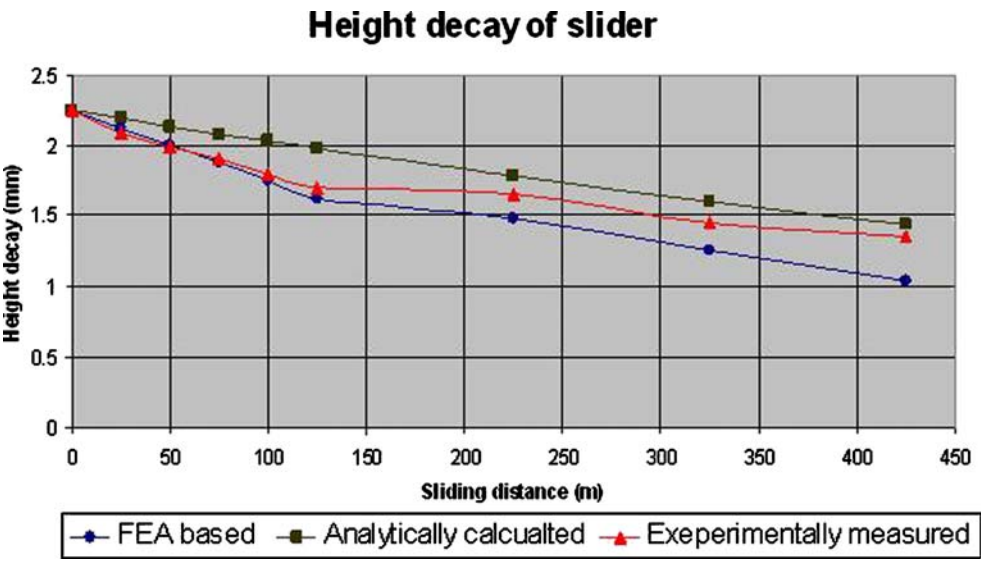

Fig. 15 Slider height decay

of target. This makes it very suitable for implementing to application like life of simulation of prosthetic joints and piston-cylinder situations. In case of meshing gears, the tooth pressure and angle rapidly varies as the gears rotate, which make the extracting of nodal pressures a difficult task. After having verified the wear simulation routine for a simple geometry, further application studies will be conducting with some of the aforementioned cases in future.

The two important outcomes expected from a wear model from engineering standpoint are: change in dimensions and localized effects of wear. The FEA model presented addresses both aspects.

Dimensional changes resulting from wear are seldom uniformly distributed, therefore any wear prediction model (analytical or FEA-based) averages the changes in dimension across the contact in consideration. The FEA model can gives wear results at nodal level which can be averaged across the contact. The height decay results presented are obtained from averaging of nodal wear.

During the tests it was assumed that normal load is equally distributed to all three contacts. In reality due to variation of geometry and faults developed during injection moulding, there are variations in the load distribution. This variation of load caused uneven wear of the contacts.

Another factor contributing to the uneven wear of contacts is the slider design, which causes the leading edge to wear at a faster rate than the trailing edge. The wear measurements were conducted on the Bases of a flat-on-flat contact, which forms the major portion of the sliding profile. However, the actual sliding profile is ramp-flat-ramp. Thus, the accuracy of the wear model can be improved if combined effects of geometry and material properties are added

It was mentioned that wear calculations are performed at the end of each contact solution, ignoring the contact states at sub-steps. The contact wave illustrated earlier shows that the sliding contact zone moves along the face of the slider within each sliding step. It can be concluded that a very small sliding step with minimum sub-steps would render better results for prediction of worn geometry. However, considering the sliding distance of the order of hundreds or thousands of meters, such accuracy would be of high computational cost. Therefore, a refined model may be practicable to be used for simulating of wear in applications like MEMS. Moreover, with the selection of appropriate sliding step, this algorithm can also be used to simulate crack propagation resulting from wear.

The height decay calculated from the FEA algorithm is higher than the actual and analytically calculated values. The algorithm calculates the height decay with a value that is averaged from the wear at contact nodes. In reality, wear is always unevenly distributed across the contact face.

Practical wear problems are influenced by a number of factors including transition of wear modes, temperature build up, and surface finish. However, it is difficult to incorporate all such factors to a single FEA wear model. Depending on the capabilities of the FEA software additional factors may be added.

Acknowledgements The authors would like to thank the Australian Research Council (ARC) and Schefenacker Vision Systems Australia (SVSA) for their support of the work

References

1. Lydersen S, Rausand M (1987) A systematic approach to accelerated life testing. Reliab Eng 18(4):285–293, DOI 10.1016/0143-8174(87)90033-3
2. Sfantos GK, Aliabadi MH (2007) Total hip arthroplasty wear simulation using the boundary element method. J Biomech 40:378–389, Medline DOI 10.1016/j.jbiomech.2005.12.015
3. Zhang WM, Meng G (2006) Friction and wear study of the hemispherical rotor bushing in a variable capacitance micromotor. Microsyst Technol 12(4):283–292, DOI 10.1007/s00542-005–0064-0
4. Williams JA (2005) Wear and wear particles - Some fundamentals. Tribol Int 38(10):863–870, DOI 10.1016/j.triboint.2005.03.007
5. Zhang WM, Meng G (2006) Numerical simulation of sliding wear between the rotor bushing and ground plane in micromotors. Sens Actuators A: Phys 126(1):15–24, DOI 10.1016/j.sna.2005.08.004
6. Podra P, Andersson S (1999) Simulating sliding wear with finite element method. Tribol Int 32(2):71–81, DOI 10.1016/S0301-679X(99)00012-2
7. Rabinowicz E (1995) Friction and wear of materials. Wiley, New York
8. Hutchings IM (1992) Tribology: friction and wear of engineering material. Edward Arnold Publishers, London
9. Kim NH, Won D, Burris D, Holtkamp B, Gessel GR, Swanson P, Sawyer WG (2005) Finite element analysis and experiments of metal/metal wear in oscillatory contacts. Wear 258:1787–1793 DOI 10.1016/j.wear.2004.12.014
10. Meng HC, Ludema KC (1999) Wear models and predictive: their form and content. Wear 181–183:443–457, DOI 10.1016/0043-1648(95)90158-2
11. Ashraf MA, Najafabadi BS, Hsu HY (2006) Wear prediction: a methodical approach. In Research in interactive design, Springer, Paris
12. Ashraf MA, Najafabadi BS, Hsu HY (2006) Surface-surface contact wear prediction using FEA. In Research in interactive design, Springer, Paris
13. Ashraf MA, Najafabadi BS, Gol O, Sugumar D (2006) "Time-to-failure" prediction for a polymer–polymer swivelling joint. Int J Adv Manuf Technol. DOI 10.1007/s00170-007-1219-1
14. Hegadekatte V, Huber N, Kraft O (2005) Finite element-based simulation of dry sliding wear. Model Simul Mater Sci Eng 13 (1):57–75, DOI 10.1088/0965-0393/13/1/005
15. Cantizano A, Carnicero A, Zavarise G (2002) Numerical simulation of wear-mechanism maps. Comput Mater Sci 25:54–60, DOI 10.1016/S0927-0256(02)00249-5
16. ANSYS user's manual for version 10.0
17. Bayer RG (2002) Wear analysis for engineers. HNB Publishers, New York
18. Ashraf MA, Najafabadi BS, Gol O, Sugumar D (2007) Finite element analysis of a polymer-polymer sliding contact for Schallamach wave and wear. Key Eng Mater 348–349:633–636